FINITE ELEMENT MODEL UPDATE OF VERY FLEXIBLE AIRCRAFT BASED ON GROUND VIBRATION TESTS

Bilal Sharqi[1] and Carlos E. S. Cesnik[2]

University of Michigan, Ann Arbor, Michigan, 48109, USA

Abstract

Ground vibration testing is typically conducted on an aircraft where the structure is supported using a suspension setup that emulates the free-flying aircraft. When the structure is very flexible, it is challenging to find a suspension system that can support the structure without influencing its dynamic response. This study investigates the computational and experimental techniques required to conduct such a ground vibration test on a very flexible aircraft. Various ground vibration tests were conducted on a very flexible aircraft with different boundary conditions and excitation sources. The finite element model of the very flexible aircraft was then updated using a model updating methodology that accounts for large deflections and flexibility of the test structure. Results are provided along with a discussion of the problem setup and sources of error. The updated finite element model is used to create a prediction for the true free-flying structural dynamics of the aircraft in the absence of a suspension contaminating the response of the structure. A validation of the ground vibration testing and finite element model updating methodologies is then performed on a very flexible flying wing. Results indicate the updated finite element model of the aircraft is able to accurately capture the free-flight response of the as-built very flexible aircraft structure.

Keywords: very flexible aircraft, ground vibration testing, finite element model updating, structural dynamics

1. Introduction

New transport aircraft designs are moving to lightweight, higher-aspect-ratio wings for higher energy efficiency and lower fuel burn. These wings pose design challenges due to their high flexibility, which causes large deflections under normal loads [1]. Ground vibration testing (GVT) [2] is a critical step in the process for assessing the structural integrity of such aircraft and ensuring their safe operation [3]. During GVT, the way an aircraft is supported determines its boundary conditions [4], and in order to simulate the real aircraft in flight, the support needs to be as close as possible to the free-flying condition [5]. In reality, a truly free boundary condition is not possible on the ground. If there is a boundary condition, there will be something external to the aircraft connected to it that will impact the response of the structure under excitation. In practice, the natural frequency associated with the support system should be separated from the lowest elastic frequency of the test structure by at least an order of magnitude. While this is already challenging for conventional, stiff aircraft, the low stiffness and low fundamental frequency of a very flexible aircraft (VFA) requires a very soft suspension system to get a reasonable separation between the structure and the support mechanism [6]. It can also become challenging, if at all possible, to find a suspension/support that has the right stiffness characteristics and can support the test structure without excessive deformation [7], [8].

Very flexible aircraft can exhibit significantly different deformed shapes during normal flight operations, resulting in different modal content for each of those shapes [9]. This shape dependence on the modal characteristics of the aircraft is a direct result of the geometrically nonlinear nature of the

[1]Postdoctoral Fellow, Department of Aerospace Engineering, bilalsh@umich.edu.

[2]Richard A. Auhll Department Chair, Clarence L. "Kelly" Johnson Collegiate Professor of Aerospace Engineering, 1320 Beal Avenue - 3000 FXB, +1(734) 764-3397, cesnik@umich.edu. **Corresponding Author**.

problem that leads to different linearized results depending on the shape about which the modal characteristics are evaluated. While the modal frequencies may be properly scaled by the geometrically nonlinear effects that are intrinsically dependent on the same material and geometric properties as its linear counterpart [10], the same cannot be necessarily said for modal damping. To properly capture either of these modal properties, testing is required of the aircraft in multiple deformed configurations representative of in-flight trim shapes or other flying shapes of interest to completely characterize its structural dynamics. A variety of numerical studies have been performed demonstrating the variation in shapes of very flexible structures based on suspension location (essentially adjusting the boundary condition) and their impact on the structure [11, 12]. However there is a lack of reported studies experimentally demonstrating the impact of the deformed shapes and the variation in the structure's response based on the shape for VFA, even though by being very flexible, different shapes can be obtained from different boundary conditions on ground settings [6].

After GVT, the finite element model (FEM) of the structure needs to be tuned or calibrated such that it better matches the as-built structure's results [13]. Updated FEM require satisfactory correlation between numerical and experimental results for the modal parameters [14]. GVT provides a unique opportunity to obtain experimental data that can be used to validate and update FEMs. This process, known as finite element model updating, involves iteratively adjusting the FEM to match the experimental data obtained during GVT [15].

This paper focuses on the application of the FEM updating methodology for VFA, the corresponding GVT under different deformed shapes, and the validation of the overall methodology on a prototypical very flexible aircraft, the X-HALE [16]. This is a scale model with the representative dynamics of a solar-powered flying wing, making the problem particularly challenging. Being very flexible and made of lightweight composite materials, the airframe presents the ideal structure to exercise GVT [6] and FEM updating [17] methodologies developed for VFA. This study also includes a validation of the GVT and FEM updating methodologies by performing a free-free GVT [18] on the X-HALE. In order to get an accurate understanding of the structural dynamics of an aircraft, a free-free GVT needs to be conducted with a very soft suspension, and address the various challenges associated with designing and performing such an experiment.

This paper is structured as: Section 2 summarizes the GVT and FEM updating methodologies that take into account the needs for VFA applications. Section 3 introduces the airframe that will be used to demonstrate the methodology and its characteristics while Section 4.1 describes the various ground vibration tests conducted on the structure to characterize it. Section 4.2 presents a discussion of the FEM updating methodology on the VFA in different deformed configurations while Section 5 contains a description of the setup and results of the free-free GVT performed on the X-HALE to validate the GVT and FEM updating methodologies. Section 6 summarizes the work done and outlines the future work that will be conducted towards improving GVT techniques for very flexible structures.

2. Methodology

2.1 Ground Vibration Testing

In typical ground vibration tests, the vehicle is suspended on soft elastic supports to simulate free-free boundary conditions [11]. Since the structure needs to be supported either with springs or with a system of bungee cords, free-free boundary conditions can be only approximated [19]. Moreover, the addition of accelerometers, the presence of a shaker and its connection to the structure, and the dynamics of the support system itself add complexity to the test and interpretation of results.

While GVT of moderately flexible aircraft can be conducted in a single, undeformed (jig) shape, a single-point characterization (for a given mass condition) may not be sufficient for calibrating the FEM of a VFA, as shown in [17]. VFA achieve different configurations during normal operations, and these configurations are significantly different from the undeformed shape on the ground. The effects of these geometry changes need to be accounted for and characterized by testing the aircraft in different deformed shapes that can be achieved, for instance, by means of multiple suspension points placed at variable locations along the span. However, if variable or multiple suspension points are used, the effect of each suspension point needs to be individually characterized and identified. The process is shown schematically in Fig. 1.

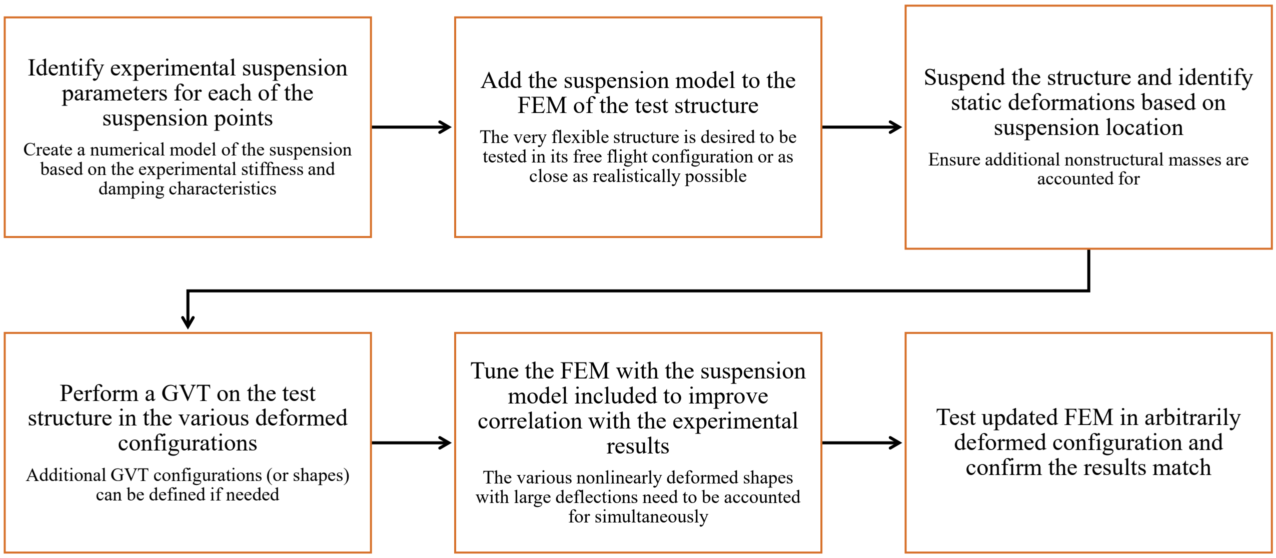

Figure 1 – Algorithm for GVT and FEM updating of very flexible structures.

2.2 Finite Element Model Updating

The typical FEM updating process is shown schematically in Fig. 2. The objective of this study was to alter the most generic FEM updating process that can handle both the mass and stiffness design variables and adapt it for very flexible structures. There can be multiple variations of the problem setup, *e.g.,* one can tune the stiffness model first using multiple deformed cases and then tune the mass model under the same load cases. However, these variations on the problem setup are not studied as part of this work.

Once GVT data is available, the FEM updating problem [17] can be cast as an optimization problem subjected to multiple nonlinear static shapes about which linearized results are obtained and compared against the GVT data. The methodology for updating the FEM of VFA is shown schematically in Fig. 3. In this process, the updated FEM obtained from the converged optimization is tested against a new set of GVT results generated within the bounds of deformation used for calibration. If the updated FEM can capture the results of the new load case within predefined tolerances, the updated FEM is retained, and the updating process concluded. If the results do not match, additional GVT data under different deformed shapes are needed. During GVT, moving the point of suspension affects the shape as well as the modal parameters in a similar manner as in-flight loads for a VFA, plus the impact of the suspensions themselves. The FEM updating process was augmented to handle multiple deformed configurations simultaneously resulting from different boundary conditions coming from different suspension configurations (as opposed to the deformations coming from a load factor), along with the suspension effects.

The optimization problem used in the FEM updating process is written as:

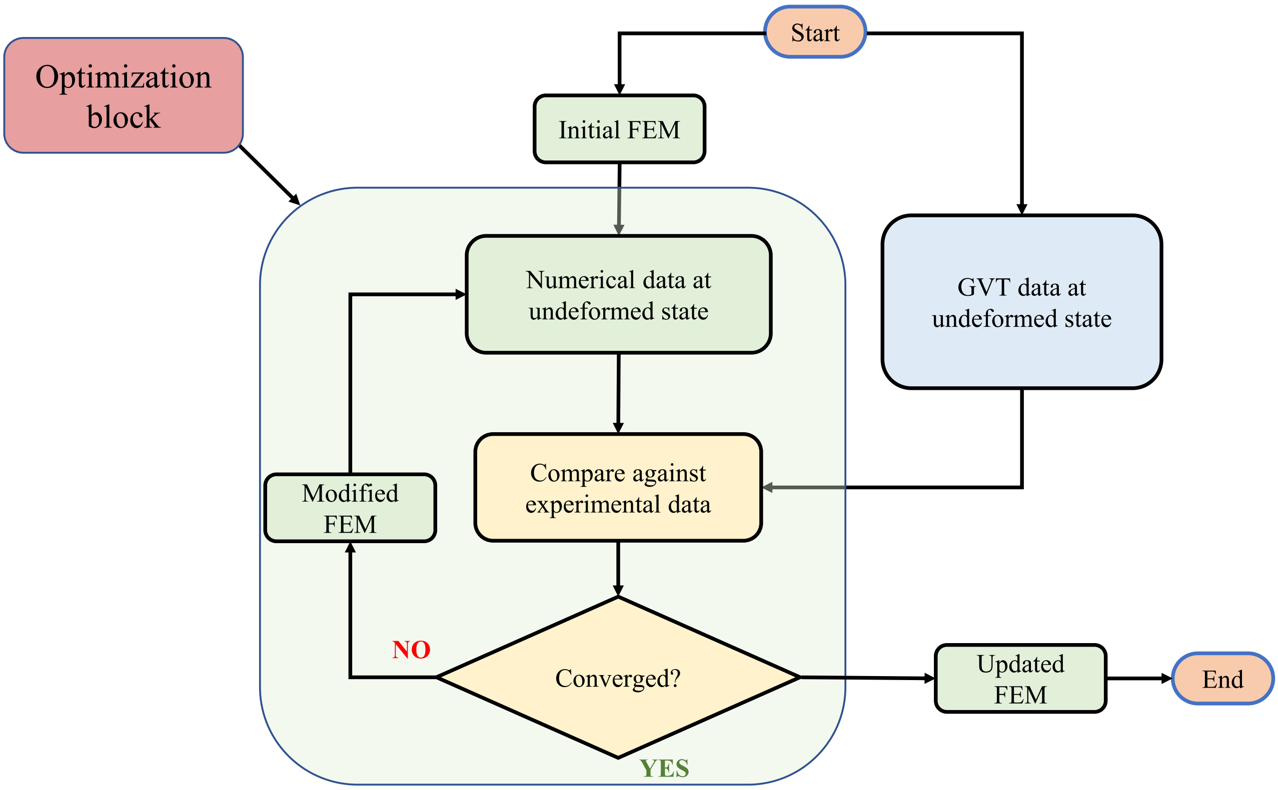

Figure 2 – Typical finite element model updating process.

$$
\begin{aligned}
\textbf{minimize F(x)} \quad &= \left(\frac{m-m_0}{m_0}\right)^2+\left(\frac{I_{xx}-I_{xx_0}}{I_{xx_0}}\right)^2+\left(\frac{I_{yy}-I_{yy_0}}{I_{yy_0}}\right)^2+\left(\frac{I_{zz}-I_{zz0}}{I_{zz0}}\right)^2+\\
&\left(\frac{X_{cg}-X_{cg_0}}{X_{cg_0}}\right)^2+\left(\frac{Y_{cg}-Y_{cg_0}}{Y_{cg_0}}\right)^2+\left(\frac{Z_{cg}-Z_{cg_0}}{Z_{cg_0}}\right)^2+\\
&\sum_{j=1}^{n}\sum_{i=1}^{N}\left(\frac{\omega_i^j-\omega_{i_0}^j}{\omega_{i_0}^j}\right)^2\\
\textbf{with respect to:} \quad & \mathbf{x}\\
\textbf{subjected to:} \quad & m^\ell \le m \le m^u\\
& I_{xx}^\ell \le I_{xx} \le I_{xx}^u\\
& I_{yy}^\ell \le I_{yy} \le I_{yy}^u\\
& I_{zz}^\ell \le I_{zz} \le I_{zz}^u\\
& X_{CG}^\ell \le X_{CG} \le X_{CG}^u\\
& Y_{CG}^\ell \le Y_{CG} \le Y_{CG}^u\\
& Z_{CG}^\ell \le Z_{CG} \le Z_{CG}^u\\
& MAC_i^j \ge MAC_{min}; \quad i=1,2,...,N \quad \text{and} \quad j=1,2,...,n\\
& \mathbf{x}^\ell \le \mathbf{x} \le \mathbf{x^u}
\end{aligned} \tag{1}
$$

where index $i=1,\ldots,N$ represents the modal number for the first N modes for each of the j^{th} deformed shape associated with the set of n shapes. The terms with the subscript o refer to the experimental value while the terms without the subscript are the corresponding numerical components. Furthermore, m is the total mass of the structure, X_{cg} through Z_{cg} refers to the three components of

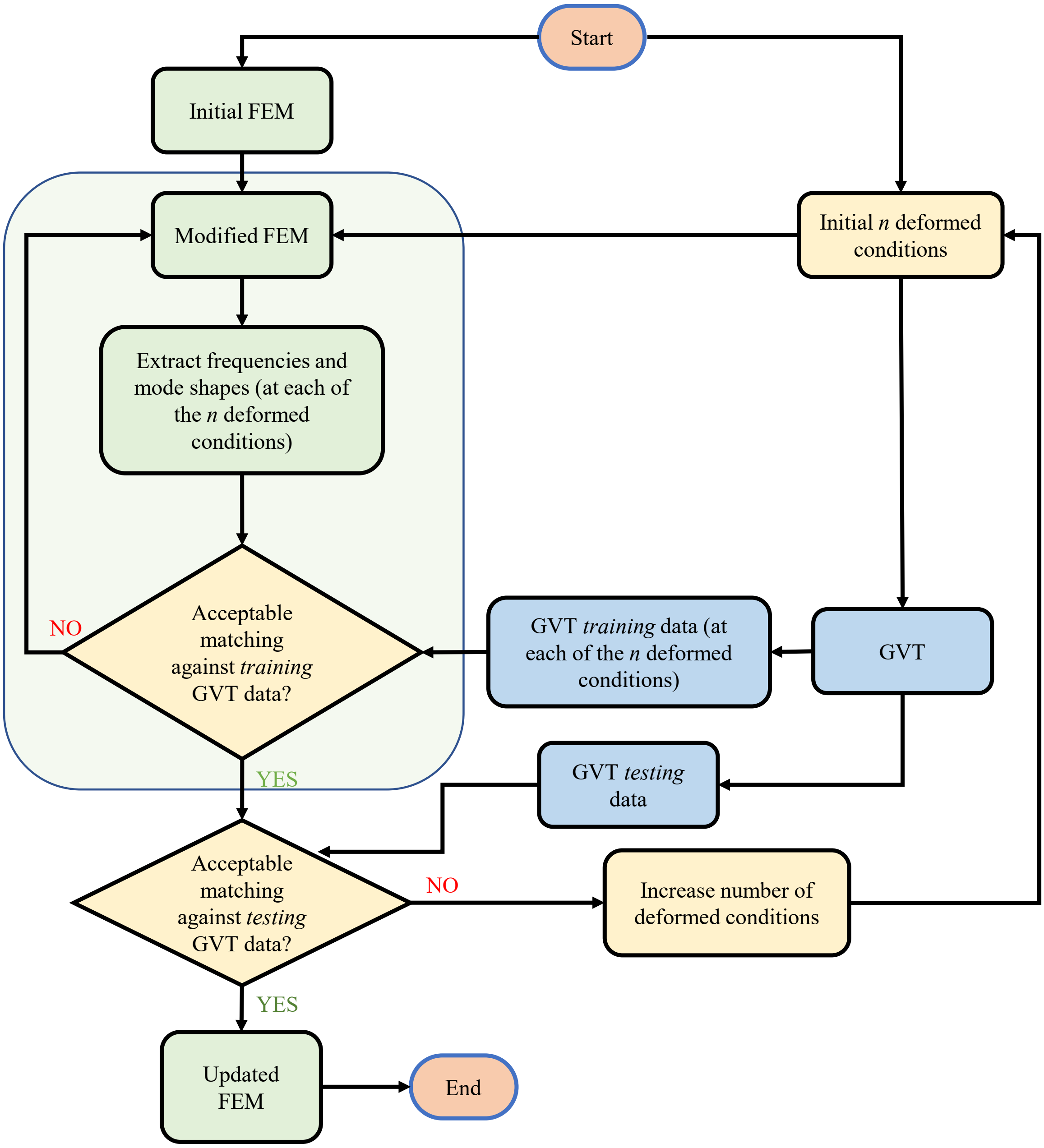

Figure 3 – Modified process for FEM updating for very flexible structures.

the center of gravity (c.g.) location, while I_{xx} through I_{zz} are the components of the inertia tensor (additional components of the inertia tensor can also be included, but are not shown or investigated here for brevity); ω_i^j is the i^{th} natural frequency associated with the j^{th} deformed shape. Finally, MAC stands for Modal Assurance Criterion [20], and MAC_{min} corresponds to the desired minimum threshold of acceptable modal correlation. The upper and lower bounds in the constraints are denoted by the superscripts u and ℓ, respectively.

3. Very Flexible Aircraft Test Case

The University of Michigan's X-HALE is an experimental testbed for identifying areas of improvement needed in design, analysis, and control of VFA [16]. The X-HALE was designed to:

1. be aeroelastically representative of VFA and exhibit nonlinear couplings between flight dynamics and structural dynamics;

2. be capable of large static deflections, with a tip deflection greater than 30% of the semi-span

during operation;

3. enable studying control design methodologies for VFA.

The X-HALE is a very flexible, remote piloted aircraft developed with the primary objective to collect experimental aeroelastic data to support code validation and to serve as a platform to evaluate control strategies. It is a wing-boom-tail type of aircraft with a 6-meter span, divided into six sections of 1-meter long each, with the tip sections set at a dihedral angle of 10 deg. The wing has an EMX-07 airfoil profile with chord of 0.2 m, while the tails have a NACA 0012 airfoil profile with a chord length of 0.12 m. There are eleven control effectors available on board the VFA: two roll spoilers located at the dihedral sections, four elevators situated at each outboard tail, and five motors providing distributed electric propulsion. The center tail is not used as a control surface.
The configuration is being experimentally studied both on the ground (GVT – discussed here) and in flight (*e.g.*, [16], [21]). These tests are building up a unique set of coupled nonlinear aeroelastic-flight dynamics data to support validation of numerical modeling, analysis and simulation tools. The X-HALE configuration can be seen both on the ground and in flight in Fig. 4, highlighting the level of deformation attained by the aircraft in flight. Its basic physical characteristics are listed in Table 1.

Figure 4 – X-HALE airframe on the ground and in flight.

Table 1 – Main X-HALE airframe characteristics.

Wing span	6	m
Wing chord	0.2	m
Planform area	1.2	m^2
Aspect ratio	30	-
Propeller diameter	0.3	m
Gross take-off weight	11.35	kg

4. Application of GVT and FEM Updating Methodologies for VFA

This section focuses on the application of the GVT and the FEM updating methodologies on the sample VFA: X-HALE. GVT were performed on the airframe in multiple deformed configurations using both an impact hammer and a shaker as excitation sources. Prior to the GVT, the suspension itself was characterized and included in the FEM, according to the methodology introduced in 2.1 A moderately stiff spring with a spring constant of 195 N/m was selected for the laboratory GVT and ten of these springs were used in series for each side of the suspension (for a net stiffness value of 19.5 N/m per set of springs). Since the total extension experienced by the ten springs is greater than the vertical height of the test facility, a single low-friction, ball-bearing pulley was used to allow the springs to extend horizontally along the length of the test rig and then turn directions (to drop vertically) in order to suspend the X-HALE. More details about the suspensions characterization and test set up are provided in [6]. Once the experimental GVT data was collected, the FEM updating process could start as shown in 2.2

4.1 GVT Results

The aircraft setup in the laboratory during GVT is shown in Fig. 5. This configuration is called “outboard” because the suspension is connected to the second (outboard) wing junctions away from the center of the aircraft. Another configuration called “inboard” was defined where the suspension is connected to the first (inboard) wing junctions away from the center of the aircraft, as shown in Fig. 6. The suspension system consisting of a series of springs and a pulley to turn directions can be seen above the aircraft. These two configurations are defined because the joint between the wings is a connection point from which the aircraft can be suspended. Moreover, using a combination of the two suspension configurations allows to recover most of the vehicle in-flight shapes. These two suspension configurations are at the extremes of the deformations the aircraft normally experiences in flight.

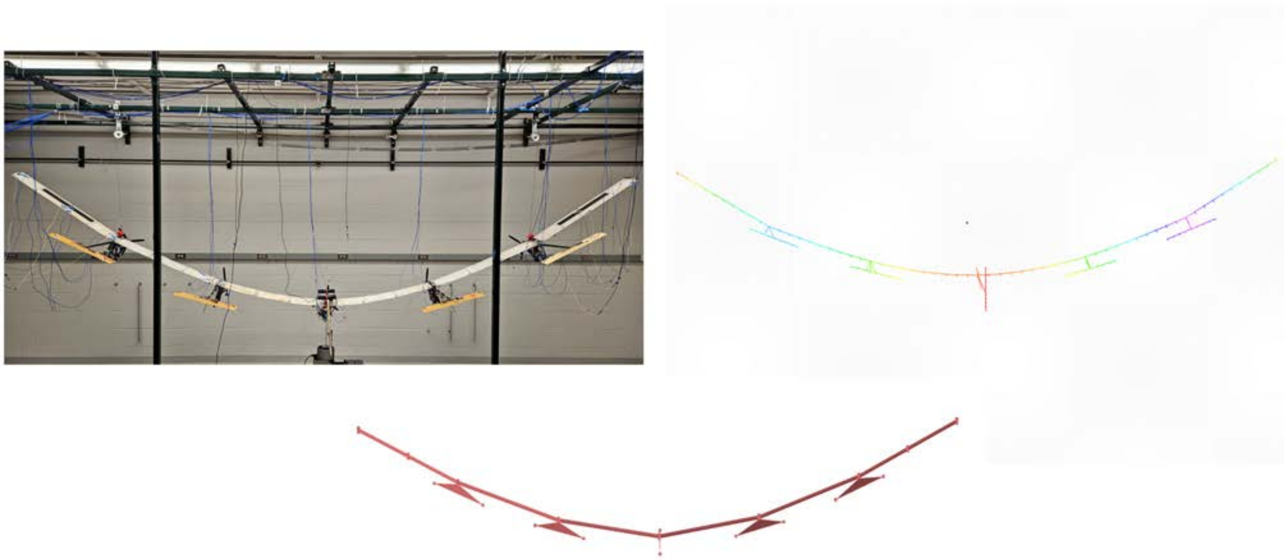

Figure 5 – The X-HALE setup for GVT in the outboard configuration (top left), the corresponding nonlinear model of the static deformed shape under self weight (top right), and the reference shape used in the test software to define the initial geometry based on the accelerometer layout (bottom).

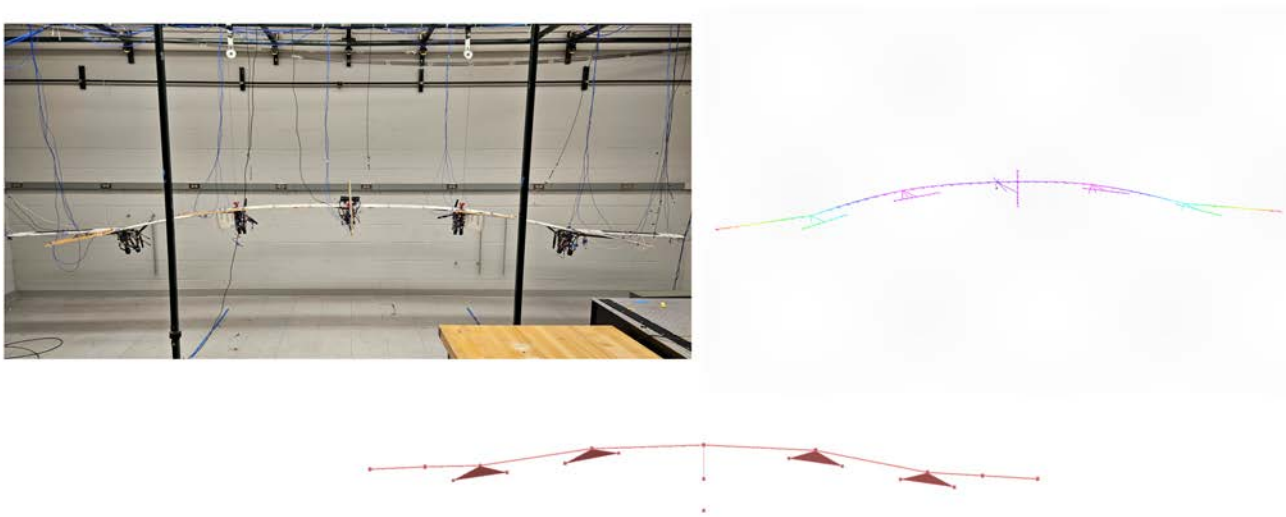

Figure 6 – The X-HALE setup for GVT in the inboard configuration (top left), the corresponding nonlinear model of the static deformed shape under self weight (top right), and the reference shape used in the test software to define the initial geometry based on the accelerometer layout (bottom).

The results from the outboard configuration laboratory GVT performed with both the shaker and impact hammer as excitation sources, compared against the FEM are summarized in Figs. 7 and 8 for the outboard and inboard configurations respectively. They indicate that while the experimental results show good agreement between themselves, there are large errors of up to 15% between the initial FEM and the GVT. The results highlight the need to update the FEM of the X-HALE considering both the configurations simultaneously.

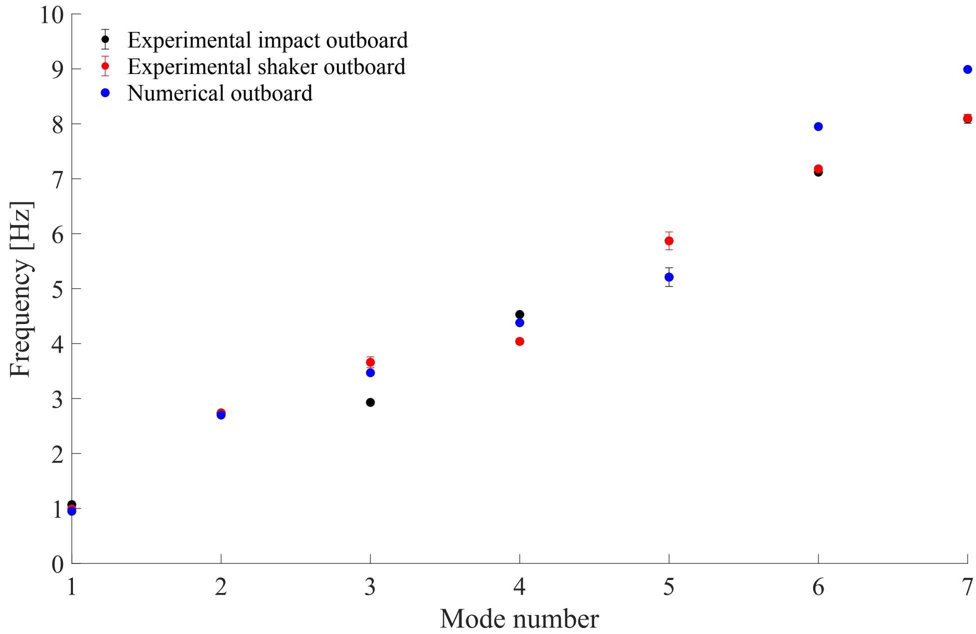

Figure 7 – Comparison of the first 7 modes from the shaker and impact hammer GVT vs. the initial FEM for the outboard configuration.

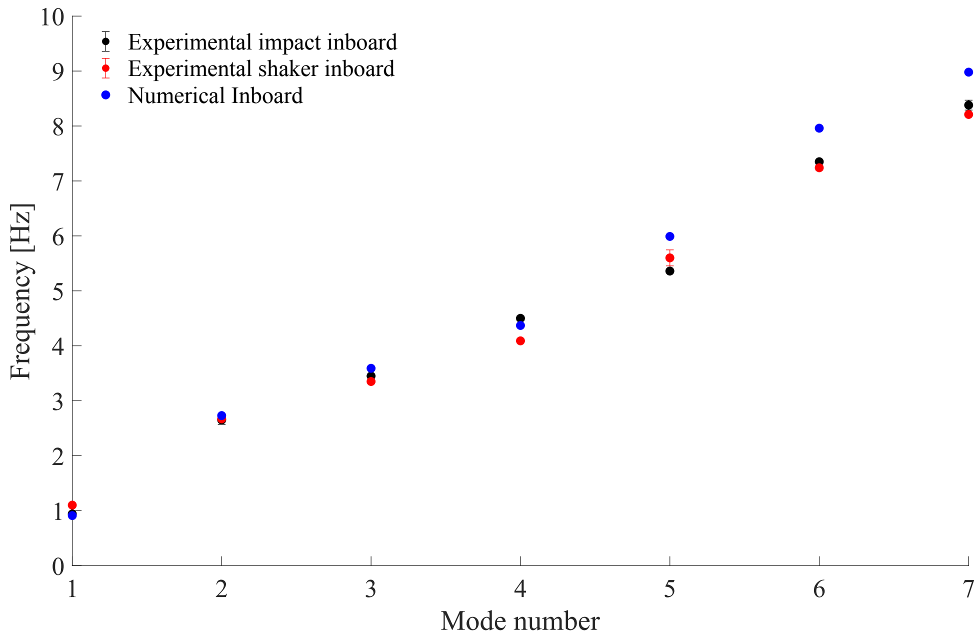

Figure 8 – Comparison of the first 7 modes from the shaker and impact hammer GVT vs. the initial FEM for the inboard configuration.

4.2 FEM Updating Results

After the GVT results become available, the VFA's FEM can be updated using the methodology described in Section 2. The FEM updating was conducted considering both the configurations (inboard and outboard) simultaneously. The errors between both configurations compared to the experimental GVT data are highlighted in Fig. 9, indicating that after the FEM updating, the first seven computational elastic modes match the experimental under 2% error.

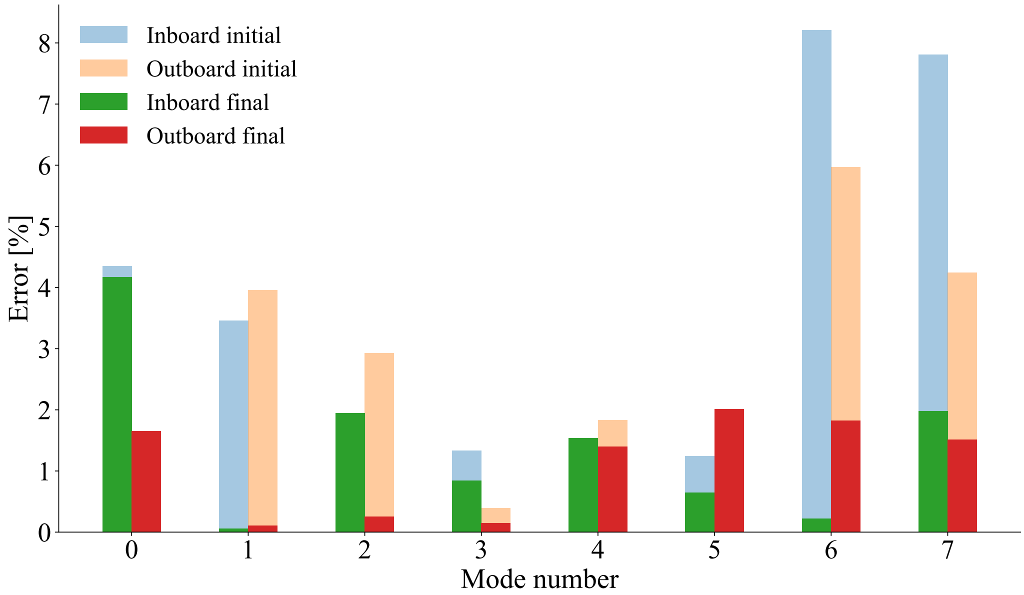

Figure 9 – Percent error after updating using GVT results compared to the initial FEM of the X-HALE for the inboard and outboard configurations. Mode 0 is the plunge mode related to the suspension.

Once the GVT and FEM updating are performed, a prediction for the true free-free natural frequencies of the X-HALE was obtained. The results are summarized in Table 2. Predictions are provided for both the “no spring" case (no suspension in the FEM), as well as a very soft bungee cord suspension used to approximate the free-free setup that will be used for validation (see Sec. 5). The largest difference between the case with no spring and the case with the very soft bungee cords is for the first elastic mode. It should also be noted that the plunge mode with this setup is predicted to be around 14% of the fundamental free-free elastic mode (first out-of-plane bending). This indicates that the suspension setup would successfully provide an order of magnitude separation between the suspension related mode and the VFA's fundamental elastic mode.

Table 2 – Predicted natural frequencies for the free-free GVT after updating the FEM.

		Frequency (Hz)				Difference (%)	
		No springs		Free-free bungee		Bungee vs. No springs	
Mode #	**Mode type**	**Inboard**	**Outboard**	**Inboard**	**Outboard**	**Inboard**	**Outboard**
0	Plunge	–	–	0.14	0.13	–	–
0	Roll	–	–	0.15	0.27	–	–
1	1 OOP	0.94	0.96	0.94	0.96	-0.2	-0.8
2	2 OOP	2.68	2.69	2.68	2.69	-0.3	0.0
3	1 T/2 IP	4.76	4.28	4.76	4.28	0.0	0.0
4	3 OOP	4.43	4.46	4.43	4.46	0.0	0.0
5	2 T/3 IP	7.04	6.27	7.04	6.27	0.0	0.0
6	4 OOP	7.21	7.19	7.21	7.19	0.0	0.0
7	5 OOP	8.25	8.26	8.25	8.26	0.0	0.0

5. Validation of Methodologies Through a Free-Free GVT

As part of characterizing the very flexible structure and validating the methodologies both for conducting GVT and updating its FEM, an experiment was designed to conduct a free-free GVT on the X-HALE. The objective is to identify true free-free modal parameters of the VFA by getting as close as possible to an order of magnitude separation between the suspension related modes and the fundamental elastic mode of the structure. This presents two challenges, which are addressed in this section.

1. Challenges related to the measurement of very low frequencies. These frequencies come from both the test structure and the suspension itself.
2. Challenges related to the suspension, i.e., obtaining a soft enough suspension to minimize interaction between the suspension modes and the aircraft's elastic modes.

In order to capture low-frequency vibrations, identifying and obtaining a sensor capable of measuring vibrations lower than 1 Hz was required. DC accelerometers are DC-coupled, and can respond down to zero Hertz. They therefore can be used to measure static as well as dynamic acceleration.

In order to minimize the influence of the support, the aircraft should be connected to a suspension system that offers an order of magnitude of separation between the suspension related rigid body modes and the structural modes associated with the aircraft. To accomplish this separation, a suspension setup made of long, low-stiffness bungee cords that would support the weight of the aircraft and remain in the linear region of deformation was designed.

A 1 m long segment of the spool of the bungee cord was tested under various loads to obtain a relation between the equivalent stiffness per unit length of the bungee cord. The mathematical relation used to create the equivalent stiffness per unit length is shown below.

$$\sigma = E\varepsilon = \frac{F}{A} \implies F = EA\varepsilon = EA\frac{\Delta l}{l} = (\frac{EA}{l})\Delta l \tag{2}$$

Since the bungee cord can be considered as an equivalent spring where the load-extension relation $F = kx$ applies in the linear region (where k is the spring constant), the term $\frac{EA}{l}$ in Eq. 2 is an analogous expression to the spring constant. For a 1 m long bungee cord, it would just be EA. The stiffness constant of the bungee cord varies inversely with its initial length. The equivalent bungee cord stiffness per unit length was verified by testing cords with varying initial lengths and identifying the slope of the load vs. extension curves. Based on the stiffness tests, for the bungee cord, a prediction can be obtained for the plunge frequency as a percentage of the fundamental free-free elastic mode of the X-HALE. A sample of this is shown in Table 3.

Table 3 – Bungee cord assessment and prediction.

Initial length [m]	Stiffness [N/m]	Plunge frequency [Hz]	Extension under ½ X-HALE [m]	Total extension [m]	Fundamental elastic mode [Hz]	Difference from true free-free 1st mode [%]	Plunge freq. as a % of fundamental free elastic mode
0	0	-	-	-	0.921	-	-
10	9.03	0.2	1.79	10.79	0.938	1.85	21.7
20	4.51	0.14	4.32	24.32	0.929	0.87	15.2
30	3.01	0.12	7.59	37.59	0.927	0.65	13.0

In order to keep the total height of the facility where the bungee cord would be deployed within reasonable limits, it can be observed that a bungee cord of approximately 20 m would provide a sufficient separation between the suspension related plunge resonance mode and the fundamental elastic mode of the X-HALE. As can be observed from Table 3, there are diminishing returns to increasing the bungee length. The increase in the separation between the suspension mode and the aircraft's elastic mode does not justify the exponential increase in both the initial bungee length and the displacement under loading. Two bungee spools of 75 ft each (22.86 m) were acquired and set up to be used with the X-HALE, with each side of the aircraft connected to one bungee cord. Even though these spools were the same part and manufactured by the same company, upon testing, it was observed that their stiffness per unit length were quite different. These differences and predicted

total lengths at the desired initial length are shown in Table 4, while a plot of the bungees' initial lengths versus cumulative extensions under the mass of the X-HALE is provided in Fig. 10.
It can be observed that the plotted cumulative extensions under the load are slightly nonlinear. This is because the mass of the bungee cord is considered in the predictions - as the initial length of the bungee cord increases, the load increases slightly because of the mass of the cord. Bungee cords may have non-uniform stiffness along their lengths, and exhibit some change in stiffness as they are used (repeated cycles of stretching). In order to account for these concerns, there needs to be a mechanism to align their stretched lengths to have the X-HALE under 1 g (self-weight) in the outboard/inboard configuration. This is required to prevent the airframe from being lopsided once connected to the bungee cords (*i.e.*, the vertical lengths of the bungee cords need to align). A prediction for the true free-free natural frequencies of the X-HALE after FEM updating is provided in Table 2.

Table 4 – Differences between, and predictions for the X-HALE bungee cords.

Bungee ID	Initial length [m]	Stiffness per unit length [N/m]	Predicted plunge frequency [Hz]	Predicted extension under X-HALE [m]	Predicted total length under X-HALE [m]
Bungee 1	20	92.5	0.129	4.2	24.2
Bungee 2	20	100	0.134	3.9	23.9
Bungee 1	23	92.5	0.119	5.1	28.1
Bungee 2	23	100	0.123	4.7	27.7

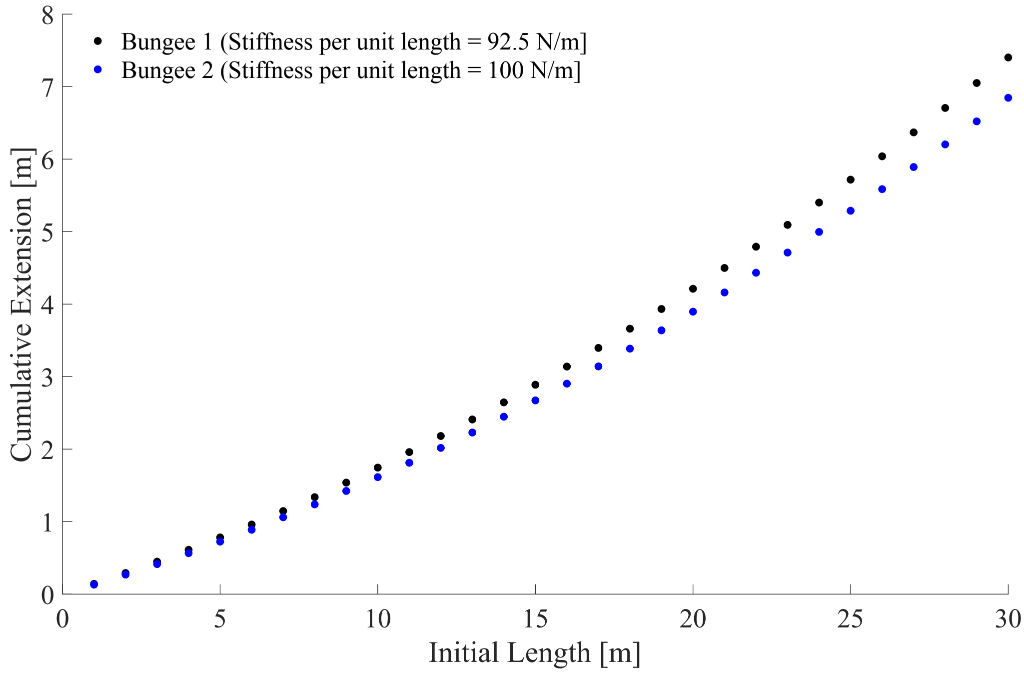

Figure 10 – The two bungee cords' initial lengths versus predicted extensions under the mass of the X-HALE.

5.1 Test Setup

The X-HALE was suspended from a crane bucket which was elevated to around 100 ft allowing the bungee cords to stretch and provide the soft suspension. The crane bucket was connected to the airframe using two bungee cords. A winching mechanism was used to attach one end of the bungee cord and allow cranking the winch to adjust the length (or height) of the bungee cord as needed. A pulley was used with a Kevlar string to turn directions such that the operator can easily access the cranking mechanism and adjust the height of each bungee individually.

A schematic with the components used is shown in Fig. 11. The crane, X-HALE and bungee cords used to approximate the free-flying conditions are shown in Fig. 12.

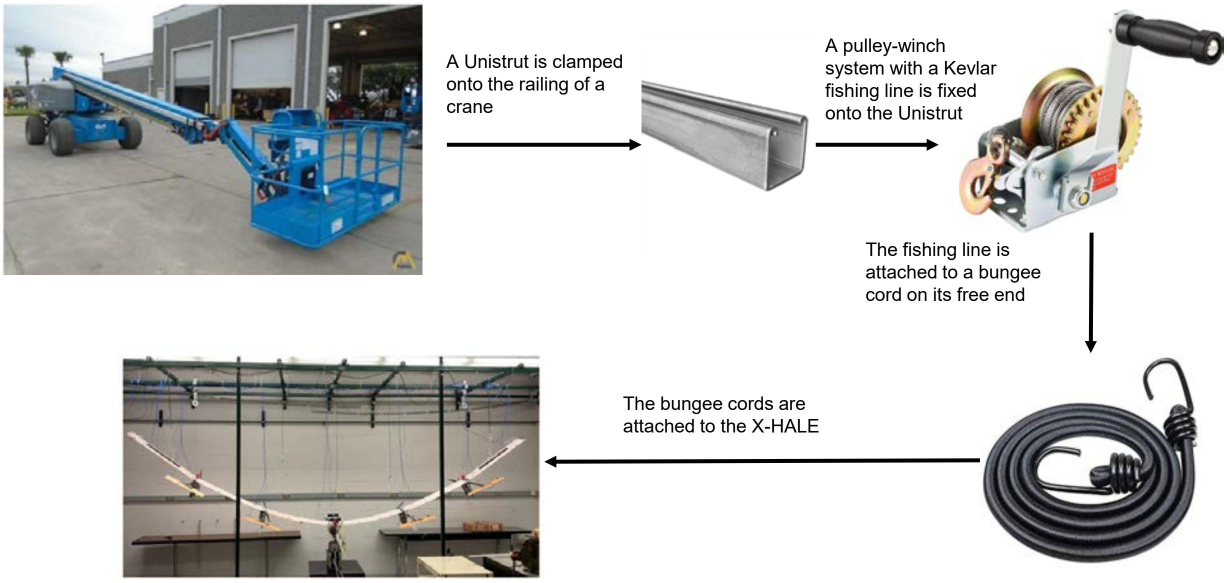

Figure 11 – Components used in the X-HALE free-free GVT.

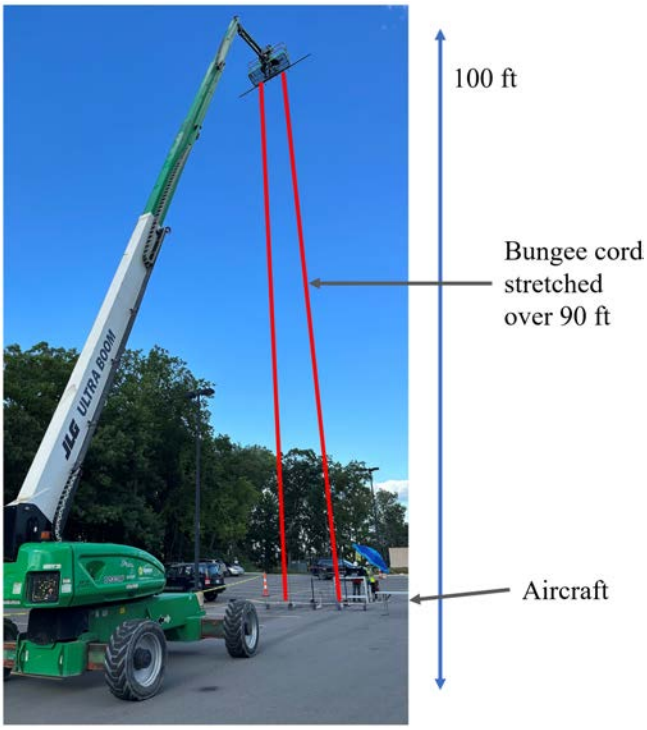

Figure 12 – The crane with the X-HALE suspended from it during the free-free GVT.

The Unistrut [3] and pulley arrangements attached to the crane were set up in a way that allowed changing the location of the bungee connections on the X-HALE, by adjusting which pulley the bungee cords dropped down from. This way, the inboard and outboard configurations could easily be swapped out, by adjusting the pulley location on the crane side, and changing the adapter position the bungee cords connect to, on the aircraft side. The X-HALE suspended from the bungee cords in the outboard configuration during the free-free GVT is shown in Fig. 13.

[3] https://www.atkore.com/About-Us/Brands/Unistrut

Figure 13 – The X-HALE suspended in the outboard configuration during the free-free GVT, connected to the bungee cords dropped from the crane.

Multiple rounds of tests were conducted in both configurations – both for statistical averaging data (and to have additional data in case of connection stiffness related uncertainties or nonlinearities), as well as collecting data in both configurations as the bungee cord gets stretched and used over the course of the experiment. The concern of the bungee cord not having uniform stiffness along their lengths and exhibiting change in their stiffness as they are used could then be accounted for by conducting these multiple configuration swaps over time, as the bungee cord gets used. The accelerometer layout for these tests included two DC accelerometers located 1.5 m away from the center of the X-HALE to measure the plunge and roll frequencies, expected to be < 0.5 Hz for both configurations. Triaxial accelerometers were installed along the quarter-chord of the wing to measure in-plane and out-of-plane bending motion, and uniaxial accelerometers were installed at multiple stations along the span. Each uniaxial station consisted of one accelerometer at the leading and trailing edges of the wing, to capture both bending and torsional motions. The accelerometer layout used for the free-free GVT on the X-HALE is shown in Fig. 14.

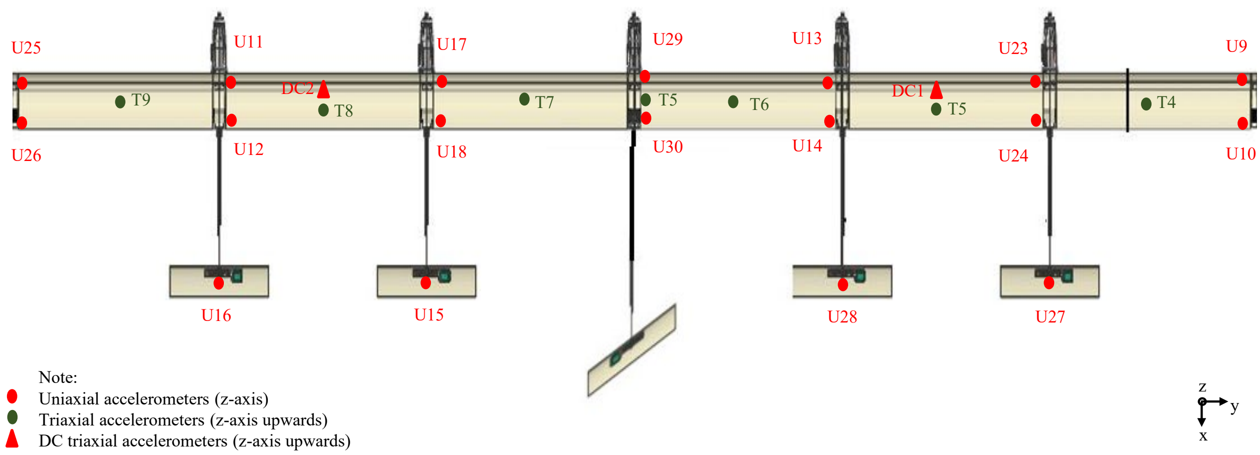

Figure 14 – Accelerometer layout for the free-free GVT on the X-HALE.

5.2 Results of the Free-Free GVT

A ground station was set up on the field for data acquisition and as the center point for all the accelerometers and instrumentation cabling to connect to. It was not possible to bring a shaker out to the field where the GVT was being conducted due to the high voltage and power requirements on the shaker and amplifier (along with the requirement to create a stable mount to bolt the shaker to the ground), only impact tests were conducted on the X-HALE during the free-free GVT. The laboratory GVT performed prior and summarized in Section 4.1indicated that impact tests provided sufficient energy to excite the modes of interest on the X-HALE. An overview of the ground station as seen from the crane is shown in Fig. 15.

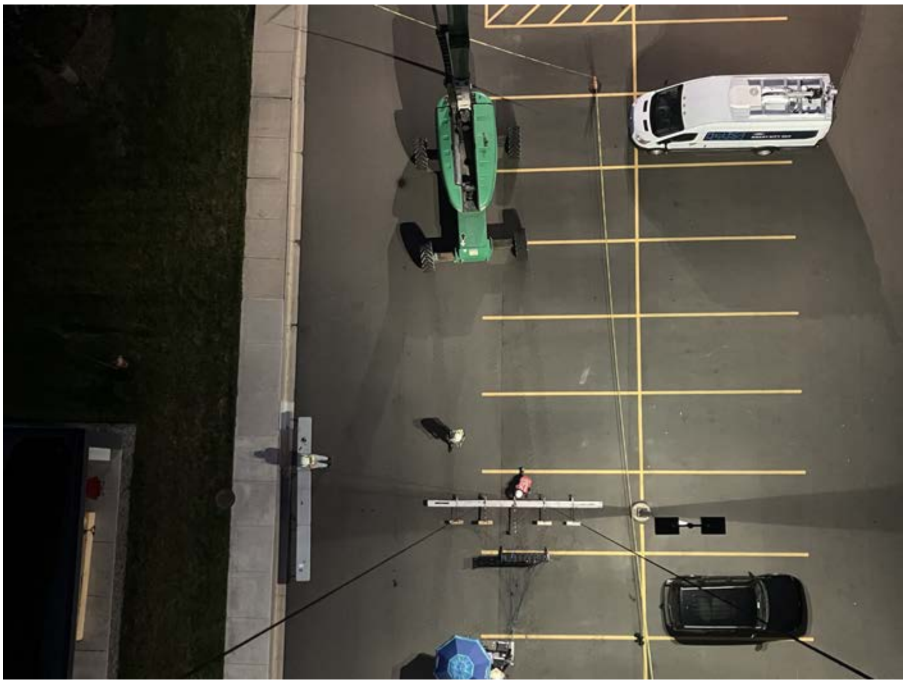

Figure 15 – The X-HALE during the free-free GVT, as viewed from the crane.

In order to identify the plunge frequency of the bungee cords with a rigid mass representative of the X-HALE (or half of the aircraft per bungee cord), a block mass was connected to the bungee cord and tested. This was done by pulling down the mass and timing the oscillations using two separate timers (operated by two people). This mass was created by using a set of adjustable dumbbells and the independent bungee excitation with this mass is shown in Fig. 16. In order to identify if the bungee cord(s) exhibited a varying stiffness with use and being stretched, these tests were conducted multiple times over the course of the free-free GVT campaign. Table 5 shows the plunge mode identified from the different bungees over the course of the test. The tests were done at each configuration change, so some of the entries are dashes, meant to represent the lack of that configuration's plunge mode being tested at that time. A similar test was done when the aircraft was suspended in both inboard and outboard configurations to measure its rigid body modes. The rigid body modes of the aircraft were tested at each configuration swap as well. The modes are the result of the bungee stiffnesses interacting with the mass/inertia of the aircraft. It is desirable to have the effect well separated from the first elastic mode — ideally the rigid body modes converge to zero Hz, but the fact that the suspension has a non-zero stiffness prevents that from being realized.

Table 6 shows the plunge and roll modes of the aircraft with the bungee suspension. It can be observed that the bungees were significantly stiffer than the initial prediction shown in the first two rows in Table 2, while being more uniform or consistent between each other. The increased uniformity comes from the fact that the bungees were characterized in the laboratory by unspooling a small segment of each of them and testing their stiffness, and not at their total length. The full-length bungees are close to each other, but random segments of the bungee cords might exhibit some non-uniformity.

Figure 16 – The calibrated mass (dumbbell suspended from bungee cord, middle of the image) used to measure the bungee plunge frequency.

Table 5 – Plunge frequencies with the block mass representing $\frac{1}{2}$ the X-HALE mass. Frequencies measured at various points during the free-free GVT to check if, and how the bungee stiffnesses change over the course of the GVT.

	Plunge frequencies in Hz		
Bungee location	**Beginning**	**Middle**	**End**
Inboard right	0.18	–	0.17
Inboard left	0.18	–	0.18
Outboard right	–	0.17	–
Outboard left	–	0.17	–

Table 6 – Rigid body modes of the X-HALE realized because of the interaction of the bungee stiffness with the aircraft's mass/inertia. Frequencies in Hz measured at various points during the free-free GVT to check how the bungee stiffnesses change over the course of the GVT.

Bungee location	**Beginning**	**Middle**	**End**
Inboard plunge	0.21	–	0.22
Inboard roll	0.22	–	0.23
Outboard plunge	–	0.20	–
Outboard roll	–	0.31	–

Since the plunge and roll tests conducted on the block mass or the X-HALE were recorded or measured using handheld timers, there are numerous sources of error associated with them. Some of them are discussed below:

- The times recorded between the different people observing the rigid body modes varied by up to 10%. This is due to multiple reasons – the manual nature of turning on or off the stopwatch, the lag or delay in response time between people as well as the subjectivity associated with counting the peaks and valleys of the block or aircraft as it plunges or rolls.
- The block mass was created based on the weight of the aircraft divided by two (one block mass supported by each bungee). However, the aircraft's mass is not symmetrically distributed along its span, and this can cause a slight difference between the rigid body modes coming from the

isolated block mass attached to the bungees compared to the X-HALE.

- The mass of the accelerometers on the aircraft was not modeled in the FEM. This creates modeling errors regarding the impact of the accelerometer mass and their cables on the aircraft.
- The summer weather melted the wax used to connect the accelerometers to the airframe. This was resolved by taping the accelerometers to the airframe, which is different than how they were attached during the laboratory GVT.
- The accelerometer wires leading away from the accelerometers (i.e., the cables in contact with the airframe) were interfering with the motion of the aircraft during the rigid-body tests. The wires were holding the plane in a non-resting position, introducing additional stiffness to the system. However, even with this increased stiffness (which is only relevant during the rigid body modes where there are large displacements of the structure), the suspension related plunge mode is sufficiently far away from the fundamental elastic mode of the X-HALE.

The results of the free-free GVT on the X-HALE, and the comparisons with the predicted data from the updated FEM are shown in Table 7, indicating a good match for the plunge and the roll modes of the aircraft, and very good matching of the first few elastic modes. The outboard configuration was observed to have lower damping in the rigid body modes (more oscillations could be observed visually before reaching equilibrium). Another observation was that the in-plane and torsion dominated modes are harder to identify in the inboard configuration. This can be improved by exciting the structure in the in-plane direction, but since some of the modes were not easily identifiable in the current tests, they are listed as missing here, represented by dashes.

Table 7 – Results of the X-HALE free-free GVT compared with updated FEM. The measured bungee stiffnesses at their full lengths were used to generate the numerical results.

		Frequency (Hz)				**Difference (%)**	
		Updated FEM		**GVT**		**Predicted Num. vs Exp.**	
Mode #	**Mode type**	**Inboard**	**Outboard**	**Inboard**	**Outboard**	**Inboard**	**Outboard**
0	Plunge	0.17	0.18	0.21	0.20	−18.0	−9.1
0	Roll	0.18	0.32	0.22	0.31	−19.2	2.5
1	1 OOP	0.94	0.97	0.95	0.98	−0.8	−0.6
2	2 OOP	2.69	2.69	2.71	2.67	−0.8	0.5
3	1 T/ 2 IP	4.76	4.28	–	4.22	–	1.3
4	3 OOP	4.43	4.46	4.49	4.46	−1.3	0.0
5	2 T/3 IP	7.04	6.27	7.04	6.36	0.0	−1.5
6	4 OOP	7.22	7.19	7.43	7.32	−2.9	−1.8
7	5 OOP	8.25	8.26	8.38	8.44	−1.5	−2.3

For reference, the initial FEM before being updated was notably worse in predicting the behavior of the X-HALE under the free-free suspension conditions. Initially, some modes were predicted within 3% error, while others had errors exceeding 5% between the FEM and the experimental results. Table 8 shows the results of the predicted modes from the initial FEM before the FEM updating compared to the experimental results from the free-free GVT.

A major source of uncertainty here that prevents a better match particularly for the rigid body modes is the fact that the accelerometer wires were interfering with the motion of the aircraft during the rigid body and impact tests. The wires were holding the plane in a non-resting position, introducing additional stiffness to the system, impacting both the rigid body and the elastic modes of the X-HALE. This is consistent with the observation in past work [6] about accelerometer cables from two sets of GVT on the same structure with different wire configurations and how they can influence the results for very flexible structures. A key takeaway from this set of tests is that cable management of the accelerometers can have a non-negligible impact on the response of very flexible structures. In order

Table 8 – Results of the X-HALE free-free GVT compared with initial FEM.

		Frequency (Hz)				Difference (%)	
		Initial FEM		GVT		Predicted Num. vs Exp.	
Mode #	**Mode type**	**Inboard**	**Outboard**	**Inboard**	**Outboard**	**Inboard**	**Outboard**
0	Plunge	0.14	0.13	0.21	0.20	−51.8	−45.8
0	Roll	0.15	0.28	0.22	0.31	−43.8	−12.2
1	1 OOP	0.91	0.93	0.95	0.98	−5.0	−5.2
2	2 OOP	2.76	2.76	2.71	2.67	1.7	2.9
3	1 T/2 IP	4.77	4.30	–	4.22	–	1.8
4	3 OOP	4.58	4.60	4.49	4.46	1.9	3.0
5	2 T/3 IP	7.03	6.15	7.04	6.36	−0.2	−3.4
6	4 OOP	7.79	7.77	7.43	7.32	4.6	5.7
7	5 OOP	8.74	8.73	8.38	8.44	4.1	3.3

to obtain more accurate results, the impact of the cables needs to be properly accounted for, by either modeling it in the FEM or by minimizing the contact between the cables and the test structure.

6. Concluding Remarks

The new methodology for updating the FEM of VFA using GVT data was applied to the prototypical example, the X-HALE. The GVT and FEM updating process was then validated using a free-free GVT. As one can see from the results presented above, the methodology was successfully able to characterize the structural dynamics of that very flexible airframe. This is an important outcome in supporting future development of high-aspect-ratio-wing aircraft for highly-efficient flight. With the GVT results used to update the FEM, it was able to match the GVT results within 2% error for the first 7 modes. For a VFA, it may not be feasible to create a suspension that allows an order of magnitude separation between the suspension modes and the fundamental elastic mode of the structure. The experimental results from the free-free GVT indicated that the FEM updated using the laboratory GVT was able to match (predict) the elastic modes of the actual structure within 2% error for the first five modes.

This work demonstrates that by properly characterizing the suspension and structure in a laboratory setting, with a suspension mechanism that does not provide the desired order of magnitude separation between its modes and the elastic modes of the main structure, we can recover enough information to fully characterize the VFA structure. Given that the behavior of the structure changes as it undergoes large deflections, different deformed shapes are needed to capture the structural dynamics behavior of such very flexible structures. The FEM updating methodology that allows to simultaneously consider multiple large deformed shapes can be applied to update the FEM, and this was demonstrated in the X-HALE. For this case, even with significant sources of error, the updated FEM was able to predict the behavior of the X-HALE. This is promising, and the results highlight the ability of the GVT and FEM updating methodology to sufficiently capture the structural dynamics behavior of the VFA without needing to conduct a full-scale free-free GVT.

7. Contact Author Email Address

mailto: cesnik@umich.edu

8. Copyright Statement

References

[1] Cesnik C. E. S, Palacios R, and Reichenbach E. Y. Reexamined structural design procedures for very flexible aircraft. *Journal of Aircraft*, 51(5):1580–1591, 2014.

[2] Giclais S, Lubrina P, Stéphan C, Böswald M, Govers Y, Ufer J, and Botargues N. New excitation signals for aircraft ground vibration testing. In *International Forum on Aeroelasticity and Structural Dynamics*, Paris, France, June 2011.

[3] Peeters B, Debille J, and Climent H. Modern solutions for ground vibration testing of small, medium and large aircraft. *SAE International Journal of Aerospace*, 1(1):732–742, August 2008.

[4] Cooley V and Giunta A. Laboratory evaluation of two advanced suspension devices for ground vibration testing of large space structures. In *AIAA/ASME/ASCE/AHS/ASC Structures, Structural Dynamics and Materials Conference*, Dallas, TX, January 1992.

[5] Pai P. F. *Highly flexible structures: modeling, computation, and experimentation*. AIAA Education Series, AIAA, 2007.

[6] Sharqi B and Cesnik C. E. S. Ground vibration testing on very flexible aircraft. In *AIAA Scitech Forum*, Orlando, FL, January 2020.

[7] Böswald M, Govers Y, Vollan A, and Basien M. Solar impulse - how to validate the numerical model of a superlight aircraft with a340 dimensions! In *Proceedings of ISMA 2010 - International Conference on Noise and Vibration Engineering*, pages 2451–2466, Leuven, Belgium, October 2010.

[8] Böswald M, Vollan A, Govers Y, and Frei P. Solar impulse – ground vibration testing and finite element model validation of a lightweight aircraft. In *International Forum of Aeroelasticity and Structural Dynamics*, Paris, France, June 2011.

[9] Palacios R and Cesnik C. E. S. *Dynamics of flexible aircraft: coupled flight mechanics, aeroelasticity, and control*. Cabridge University Press, 2023.

[10] Wan Z and Cesnik C. E. S. Geometrically nonlinear aeroelastic scaling for very flexible aircraft. *AIAA Journal*, 52(10):2251–2260, 2014.

[11] Chang C.-S and Hodges D. H. Parametric studies on ground vibration test modeling for highly flexible aircraft. *Journal of Aircraft*, 44(6):2049–2059, November 2007.

[12] Carne T. G, Griffith D. T, and Casias M. E. Support conditions for experimental modal analysis. *Sound and Vibration*, 41(6):10–16, June 2007.

[13] Covioli J. V and Coppotelli G. Experimental and operational modal analysis in support of modal model updating - a test case. In *8th IOMAC - International Operational Modal Analysis Conference, Proceedings*, pages 283–293, October 2019.

[14] Mezzapesa S, Arras M, Coppotelli G, Miller J, Valyou D. N, and Marzocca P. Correlation and updating of an unmanned aerial vehicle finite element model. In *56th AIAA/ASCE/AHS/ASC Structures, Structural Dynamics, and Materials Conference*, Kissimmee, FL, January 2015.

[15] Lung S.-F and Pak C.-G. Updating the finite element model of the aerostructures test wing using ground vibration test data. In *50th AIAA/ASME/ASCE/AHS/ASC Structures, Structural Dynamics, and Materials Conference*, Palm Springs, CA, May 2009.

[16] Cesnik C. E. S, Senatore P. J, Su W, Atkins E. M, and Shearer C. M. X-HALE: A very flexible unmanned aerial vehicle for nonlinear aeroelastic tests. *AIAA Journal*, 50(12):2820–2833, 2012.

[17] Sharqi B and Cesnik C. E. S. Finite element model updating for very flexible wings. *Journal of Aircraft*, 60(2):476–489, March-April 2023.

[18] Carne T. G, Griffith D. T, and Casias M. E. Support conditions for free boundary-condition modal testing. *Conference Proceedings of the Society for Experimental Mechanics Series*, 2007.

[19] Gupta A, J. Seiler P, and Danowsky B. Ground vibration tests on a flexible flying wing aircraft. In *AIAA Atmospheric Flight Mechanics Conference*, San Diego, CA, January 2016. AIAA 2016-1753.

[20] Pastor M, Binda M, and Harčarik T. Modal assurance criterion. *Procedia Engineering*, 48:543–548, 2012.

[21] Jones J. R and Cesnik C. E. S. Preliminary flight test correlations of the X-HALE aeroelastic experiment. *Aeronautical Journal*, 119(1217):855–870, 2015.